The effect of shear and confinement on the buckling of particle-laden interfaces

2016 J. Phys.: Condens. Matter 28 025101

(http://iopscience.iop.org/0953-8984/28/2/025101)

IOP Publishing Journal of Physics: Condensed Matter

J. Phys.: Condens. Matter **28** (2016) 025101 (11pp) doi:10.1088/0953-8984/28/2/025101

The effect of shear and confinement on the buckling of particle-laden interfaces

Theo D Kassuga and Jonathan P Rothstein

Department of Mechanical and Industrial Engineering, University of Massachusetts – Amherst, 160 Governors Drive, Amherst, MA 01003, USA

E-mail: rothstein@ecs.umass.edu

Received 14 September 2015, revised 3 November 2015
Accepted for publication 19 November 2015
Published 11 December 2015

Abstract

In this paper, we investigate the buckling of an air–water interface populated by lycopodium powder particles using a specially designed Langmuir trough with side walls that deformed affinely with the particle-laden interface in order to minimize the effect of shear during compression. Confinement effects from the side walls were studied by systematically reducing the width of the Langmuir trough and measuring the buckling wavelength. For interfaces wider than 20 mm, the bulk wavelength was found to be independent of interface width. Due to the presence of contact line friction along the sidewall, the amplitude and wavelength of the wrinkles near the side walls were found to be reduced by a factor two compared with the bulk. A cascade in wavelength was observed as one moved from the center of the particle-laden interface towards the sidewalls similar to what has been observed for thin floating polymer films. For interface widths less than 20 mm, the wavelength of the wrinkles in the bulk was found to decrease eventually approaching the wavelength measured along the side walls. The wavelength at the walls was not affected by confinement. At large compressive strains, a transition from wrinkles to folds was observed. These regions of strain localization formed as a train of folds shortly after the onset of wrinkling and grew in amplitude with increasing compression. Confinement was also found to have an impact on folding. To study the impact of shear during interface compression, a series of objects including circular cylinders and rectangular prisms were placed through the center of the particle-laden interface before compression. These objects enhanced wrinkling and folding upstream of the object, eliminated wrinkling and folding in a broad region downstream of the object, and realigned the wrinkles along the side of the immobile obstacles where shear strains were maximum.

Keywords: particle laden interface, buckling, confinement

(Some figures may appear in colour only in the online journal)

1. Introduction

Particle-laden interfaces have found broad application and use in a wide range of modern industries. These applications include, but are not limited to, use in consumer products, cosmetics, pharmaceuticals and foods [1]. Of particular interest is the ability of particles present on a fluid-fluid interface to stabilize emulsions. It is in this role as a Pickering emulsion [2] that particle-laden interfaces have found great commercial success and where research has been focused for more than a hundred years.

There are a number of factors that lead to the ability of particles to stabilize emulsions including the particles' wettability, shape, concentration and charge. For spherical particles, the energy needed to remove a particle from the interface between the two liquid phases is given by

$$E = \pi r_p^2 \sigma (1 \pm \cos\theta)^2, \quad (1)$$

where r_p is the radius of the particle, σ is the interfacial tension and θ is the contact angle. In equation (1), the positive sign corresponds to the removal of the particle into the continuous

phase and the minus is for the removal of the particle into the dispersed phase [3]. For colloidal particles, once they have adsorbed onto an interface, the energy required to remove a particle from an interface can be thousands of times the thermal energy. As a result, coalescence between droplets within the emulsion are hindered by the presence of the solid particles on the interfaces. Even without coalescence, Ostwald ripening can drive the disperse phase from small droplets to larger droplets within the emulsion [4]. However, the presence of particles on the interface can slow and eventually stop Ostwald ripening as the surface coverage ratio of shrinking drops becomes progressively larger, the surface tension decreases, and the Laplace pressure within the droplets of different size equilibrates [4]. Finally, it has also been suggested that the large interfacial viscosity and the interfacial elasticity which results from the presence of particles on the interface of the droplets can also affect ripening by resisting compression of the drop interface [1]. It is the interfacial elasticity of particle-laden interfaces which we will investigate in this paper.

Due to their stability, self-assembly of particles at interfaces can be used to create capsule of different shapes and sizes [5, 6] that can be used for encapsulation of pharmaceuticals, nutrients, flavors or aromas [7]. To understand the limits and the possibilities of particle-laden interfaces, it is important to investigate the basic question of how particles assemble and interact on the interface and how the properties of the resulting interface are affected by the resulting particle packing. On a very basiclevel, particles interact through long and short range forces, which can be either repulsive or attractive. Because a number of forces are at play at any given time (gravity, surface tension, Coulombic attraction and repulsion, electrodipping, van der Waals, etc) and they depend on a number of factors including the distance between the particles [8], it is natural to expect that the nature of these interactions can change as the packing of particles is modified.

Capillary interactions between multiple objects floating on an interface can lead to their self-assembly and the formation of particle rafts [9–15]. For a dense object with a large contact angle floating on the surface of a liquid, the weight of the particle can deform the fluid interface downward in such a way that the gravitational potential energy has been shown to decrease as the objects approach [16]. The result is an attractive force which scales like the inverse of particle separation and causes the floating objects to self-assemble [14–16]. For colloidal particles less than 10 μm, the weight of the particle has been shown to become too small to significantly deform the fluid interface and the gravitational forces become inconsequential [16]. It is important to note, that even in the absence of gravity, attractive interactions between particles have been observed [17]. Here we focus on particles large enough ($d = 31$ μm) to deform the interface through gravitational forces. These attractive interactions can result in particle aggregation into dense non-uniform clusters [18]. In order to assemble the particles into a well-ordered crystalline lattice, long-range attractive interactions between particles must be coupled with short-range repulsive interactions, typically from Coulomb interactions tangent to the air–water interface [19–21].

The end result of these complex particle–particle interactions is that particle-laden interfaces can have very interesting elastic behavior, particularly in shear and compression. In fact, the elasticity of the interface has been measured in a number of ways, such as by compression of flat interfaces [10] or by measuring surface pressure isotherms in particle-laden droplets [22]. Furthermore, as the interface is compressed the packing density increases and eventually reaches a maximum where particles can no longer rearrange on the interface. At this point, the surface tension goes to zero, as the repulsive and attractive interactions cancel each other [22, 23]. Because the particles cannot rearrange, further compression of the interface must either lead to compressive deformation of the particles themselves or out-of-plane deformation such as buckling of the interface [24]. Whether an interface buckles depends on whether, at a given strain, it is energetically more favorable to accommodate further deformation with additional in-plane strain or through local bending and surface wrinkles. Given that the particles tend to be relatively stiff and the resistance to bending of the interface relatively small, a particle-laden interface will usually buckle given enough strain [10, 19, 24]. The phenomena of buckling has been employed in previous work [10] to study the mechanical properties of the particle raft. A theoretical model of the buckling of particle-laden interfaces was presented in the same work [10] which showed that the wavelength of buckling is proportional to the square root of the particle diameter, $\lambda \propto d^{1/2}$. The model of Vella *et al* [10] has been shown to capture the right scaling for both air–water and oil–water interfaces and over a wide range of particle diameters above 1 μm [10, 19, 24, 25]. In this work, we will investigate how the finite size of the particle raft, confinement effects and the presence of shear can affect the wavelength and orientation of buckling.

Due to the non-uniformity of particle surface coverage and the presence of surface tension at the edge of particle rafts and along grain boundaries within the raft itself the buckling wavelength can vary quite a bit across a particle-laden interface [24]. Near the edge of the particle-laden interface and in regions of low surface coverage, surface tension has been shown to reduce the observed wavelength of the wrinkles [24]. Similar observations have been made for thin elastic sheets floating on the surface of water and other liquids. For elastic sheets, the wavelength of wrinkling has been shown to decay smoothly as one moves from the center of the sheet to its border, in a phenomenon called cascading [26]. The scaling for wavelength as a function of distance from the edge of the sheet depends on the relative magnitude of the tension that the sheet is under [27]. Recent work with particle-laden interfaces has shown that the variation and complexity of the wrinkle transitions are even richer than those observed for thin elastic films [24]. In this paper, we will investigate how confinement can affect the cascading of particle-laden interfaces.

One of the challenges to making experimental measurements of particle-laden interfaces in a Langmuir trough is the presence of the side wall of the trough which can introduce a non-trivial amount of shear during an interface compression. This shear can greatly affect the onset conditions, wavelength and orientation of buckling [24, 28, 29]. The shear originates in

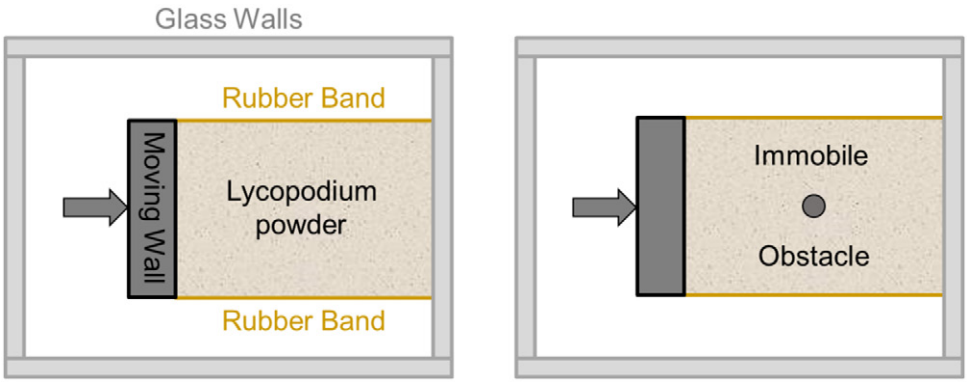

Figure 1. Schematic diagram of the modified Langmuir trough that was used in these experiments with and without the presence of an immobile obstacle sticking though the center of the particle-laden interface to introduce shear.

the boundary conditions along the side walls of the Langmuir trough. The compressive strain is imposed on one wall of the Langmuir trough. Ideally, the entire interface would experience the same compressive strain, but due to surface roughness and interactions between the particles and the side wall, interfacial shear can arise as the particles in the center of the Langmuir trough are displaced and the particles near the wall are not. These effects are accentuated as the strain and particle concentration on the interface increases causing the particle-laden interface to expand towards and push against the sidewalls as a result of the Poisson effect. This can put the contact between the sidewalls and the neighboring particles under compressive stress and increase the frictional forces between the particles and the sidewalls of the Langmuir trough. In fact, Cicuta *et al* [28, 29] showed that the displacement of a protein- or particle-laden the interface decays exponentially from a maximum displacement at the center of the Langmuir trough, where the displacement is essentially uniform, to a minimum displacement along the stationary side wall. They demonstrated that this observed deviation can be explained by friction between the particles at the interface and the stationary side walls of the Langmuir trough. Through measurements of the surface pressure isotherm, they demonstrated that increased confinement can lead to the onset of buckling smaller strains and lower surface pressures [28, 29]. Here we will attempt to eliminate the shear along the particle-laden interface which has led to the previously observed confinement effects.

One way to mitigate the effects of shear when studying the buckling of particle-laden interfaces is to redesign the Langmuir trough in such a way as to induce much larger strains in the center of the interface than near the side walls [24]. However, even though the effects of shear are reduced in Kassuga *et al*'s design [24], they are not eliminated completely and the effects of shear can still be observed especially near the corners of the Langmuir trough's moving wall. A more general method to eliminate shear is proposed in this paper. Specifically, the sidewalls are designed such that they deform affinely with the particle-laden interface. As a result, everywhere along the interface experiences the same compressive strain while at the same time the major source of shear strain is eliminated. Details of the Langmuir trough design will be presented in the following section. By eliminating shear, the design of the Langmuir trough allowed us to study the importance of shear by first removing it altogether and then systematically imposing a controlled amount of shear back to the interface and studying its effects. In the absence of shear, we will present measurements that show that side wall confinement can have a strong effect on the buckling transition and resulting buckling wavelength. Additionally, in the absence of shear, we will show that, similar to thin elastic films, strain localizations or folds can form on the buckled particle-laden interface at large strains with the number of folds increasing with increasing strain. Next, shear was imposed on the particle-laden interface by placing a series of different shaped immobile obstacles through the interface. Obstructions with circular and rectangular cross sections were employed to pierce the interface and introduce interfacial shear during compression between the moving walls and the immobile obstacle. The resulting buckling and folding patterns not only demonstrate the influence of shear along the sidewalls of the obstacles, but shielding effects that the presence of the obstacle can have on the interface downstream of the obstacle.

2. Experimental setup

The experiments were performed using a specially designed Langmuir trough shown schematically in figure 1. The three stationary walls of the Langmuir trough were glass while the moving wall was constructed of aluminum with perforations below the level of the liquid so that the liquid could flow through the wall as it moved and minimally disturb the interface. To insure a similar contact angle on all of the walls, the glass and aluminum were coated with a thin layer of Styrofoam. The entire Langmuir trough was attached to a moving stage and the aluminum wall was mounted to an optical table such that, by operating the moving stage, the Langmuir trough was moved in relation to the aluminum wall. Using the motorized stage, both the strain and strain rate were precisely controlled, but to insure accuracy, both the strain and strain rates were also independently measured from images and movies taken during and after the interface compression.

In order to mitigate the effects of shear when studying the buckling of particle-laden interfaces, the standard Langmuir trough was redesigned such that the side walls would deform

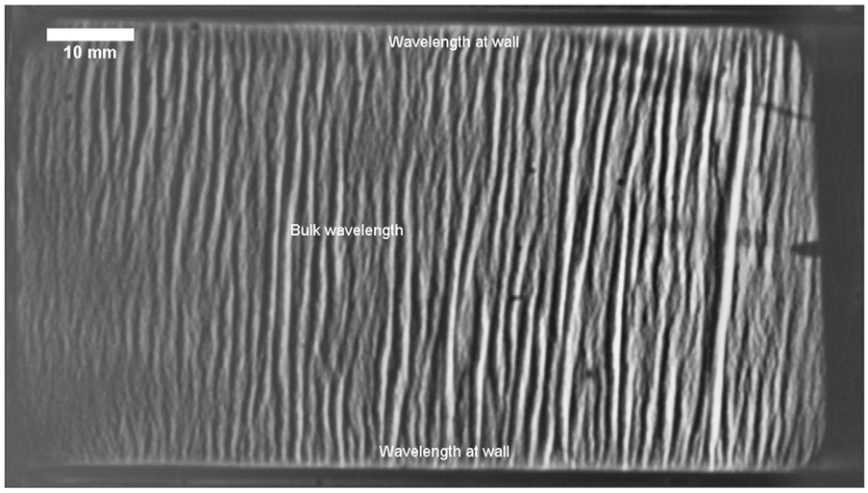

Figure 2. Representational example of a lycopodium powder populated water interface under compression. The initial dimensions of the interface were 125 mm long and 51 mm wide. In the image, the interface has been compressed by 20% and buckled. To minimize shear, the top and bottom walls are fabricated from rubber bands which deform affinely with the interface. The bulk wavelength is measured in the center of the interface while cascading can clearly be seen near the top and bottom walls.

affinely with the particle-laden interface. To accomplish this, the side walls of the modified Langmuir trough were fabricated from thin strips of highly elastic latex sheets, i.e. rubber bands. The rubber bands (Charles Leonard Inc.) were 6.35 mm wide and 0.8 mm thick and variable length depending on the experimental setup, but typically 50 mm. The rubber bands were attached to the moving wall and to the opposite side of the Langmuir trough in order to create a rectangular particle-laden interface 125 mm long with variable width. At the beginning of an experiment, the rubber bands were pre-tensioned by stretching them from their original length to 125 mm, before forming the particle-laden interface. As a result, when the particle-laden interface was at 0% compressive strain and completely relaxed, the rubber bands were at maximum extension and under maximum tension. During an experiment, as the moving wall compressed the particle-laden interface, the compressive strain on the interface increased as the tensile strain on the rubber bands decreased. As long as the strain imposed during pre-tensioning of the rubber bands was larger than the maximum compressive strain imposed upon the interface, the rubber band walls remained straight, moved affinely with the interface, and most importantly imposed no shear on the interface. For the experiments with rectangular interfaces, eight different interface widths were studied to understand the importance of confinement effects: 6.5, 10.9, 12.7, 13.5, 22.5, 30.0, 51.0 and 66.9 mm.

Shear was re-introduced into the experiments by placing an immobile obstacle through the particle-laden interface and compressing the interface around it. Both a cylindrical and a rectangular obstacle made from acrylic were used and initially placed at the center of a clean air–water interface prior to the addition of particles as shown in figure 1. The cylinder measured 5 mm in diameter while the rectangle was 10 mm $\times$ 3 mm and aligned at 0°, 45° and 90° to the compression direction.

The particle-laden interfaces were generated by sprinkling hydrophobic lycopodium powder (Carolina), $d = 31$ μm, on top of the air–water interface once the initial Langmuir trough geometry was set. Excess particles were removed by gently blowing across the surfaces using a plastic transfer pipette. Lycopodium particles are not perfectly monodisperse with a 7% coefficient of variation on the diameter and are not perfectly spherical, but have a more bullet-like shape with a circularity of 0.94 as measured on a Nikon TE2000-U optical microscope. Even so, interfaces formed with lycopodium powder are known to become elastic at high concentrations and buckle under sufficient compression with wavelengths just below 2 mm which are easily observed optically [24].

3. Results and discussion

3.1. Effect of confinement on buckling and cascading

A series of rectangular particle-laden interfaces with different widths were generated and systematically compressed by as much as 40% strain in order to investigate the role of confinement on the buckling wavelength and the cascading. An example of a buckled particle-laden interface is shown in figure 2. In figure 2, a rectangular lycopodium powder interface initially 51 mm wide and 125 mm long has been compressed by 20%. The resulting buckling patterns and transitions can be clearly observed across the interface with large wavelength buckles aligned normal to the compression direction appearing near the center of the film. As one moves closer to the edge of the interface, one can see a cascade from the bulk wavelength to smaller wavelengths similar to recent measurements with particle-laden interfaces [24] and thin elastic membranes [26, 27, 30–34].

In our experiments, buckling tended to initiate at approximately 10% compressive strain along the walls before appearing in the center of the interface with increasing compressive strain. This is likely because it is energetically more favorable for particles to aggregate nears the walls where the initial mean curvature of the interface is non-zero. The curvature along the walls is due to a contact angle between the

water and the walls which is not exactly 90°. Zeng *et al* [35] studied the interface deformation that occurs when a spherical particle adsorbs to a cylindrical interface. Unlike on a flat interface, when a spherical particle adsorbs to a curved interface, the constant contact angle condition cannot be met without deforming the interface. Zeng *et al* [35] showed that the resulting interface deformation has quadrupolar symmetry with the interface around the spherical particle being raised along the axis of the cylinder axis and depressed along the azimuthal direction of the cylinder. They also demonstrated that two spheres on a curved liquid interface will be driven by a curvature-capillary force to areas with more negative Gaussian curvature. As a result, a higher initial concentration of particles is expected along the walls of the Langmuir trough where the interface shape is cylindrical. The higher initial concentration results in a lower critical strain for buckling because less interface compression is required to bring the particles to maximum packing.

The appearance of a cascade in the buckling wavelength in figure 2 from approximately 2 mm in the bulk to 1 mm along the wall, was not unexpected as it has recently been reported for particle-laden interfaces [24], however, the origin of the cascade was not initially obvious. For elastic sheets floating on the surface of a liquid, the interfacial tension of the liquid acts on the edge of the floating sheet adding an additional tensile stress which resists large amplitude, out of plane deformation of the elastic sheet and reduces the wavelength of buckling near the edge of the sheet [32]. Given the mobility of particles on a liquid interface, the formation of a sharp edge to the particle raft where surface tension can act is not possible. In Kassuga and Rothstein [24], they postulated that the observed cascading of the wrinkles resulted from regions of low particle surface coverage near the edge of the particle raft or in regions within the particle-laden interface that were particle poor due to the initial loading. In figure 2, a number of flat regions that have not buckled within the center of the interface can be observed at this strain. These regions show a smooth transition from the bulk wavelength to the flat unbuckled interface through a series of splits from one wrinkle to two. Similar transitions have been observed previously [24]. These flat areas are particle poor regions of the sheet, an assertion that is supported by the observation that they will typically buckle when sufficient additional compressive strain is applied. These arguments, however, do not explain the appearance of the low wavelength wrinkles on edge of the sheet where particle-laden interface meets the deformable rubber sidewall.

The change in buckling wavelength near the sidewalls does not appear to be the result of low particle concentration. As we have already discussed, the initial interface particle concentration appears to be larger near the side walls than in the bulk as a result of interface curvature. Additionally, this is likely not a result of shear as side walls are designed to compress affinely with the interface to essentially eliminate the effect of shear. The most likely cause of reduced wavelength near the side walls is friction. The source of the friction could be many fold, but here we argue that the most likely source is due to contact angle hysteresis. Due to the presence of surface roughness or chemical heterogeneity, a liquid can wet a solid with a range

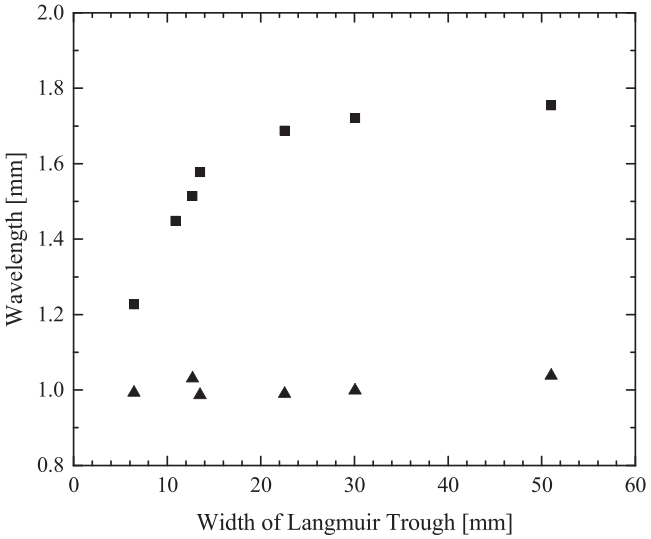

Figure 3. Average bulk wavelength (squares) and wavelength near the side walls (triangles) as a function of the width of the rectangular interface. All particle-laden interfaces were initially 125 mm long and all measurements were performed at a compressive strain 20%.

of contact angles between the receding contact angle, θ_R, and the advancing contact angle, θ_A [36, 37]. As a result of contact angle hysteresis, before a liquid drop for instance can move along a surface, the leading edge of the drop must deform to reach the advancing contact angle and the trailing edge much deform to reach the receding contact angle. A similar analysis holds for an initially straight contact line transforming into a sine wave. One can explicitly calculate the line force required to deform the water interface into the sinusoid during buckling

$$F \propto \sigma H \ (\cos\theta_R - \cos\theta_A) \ L/\lambda. \tag{2}$$

Here, H is the amplitude of the sine wave, λ is the wrinkling wavelength and L is the length of the interface just prior to buckling. Once buckled, the interface is assumed to be incompressible and inextensible. Thus, the amplitude and the wavelength are bound by a geometrical constraint which holds that the path length along the sinusoidal wrinkles must be constant independent of wavelength or compressive strain. As a result, if the buckling wavelength is reduced by two, as it is in figure 2, then the amplitude of the sine wave must also be reduced by the same factor of two. A significant consequence of this geometric constraint is that the contact line friction from equation (2) can be shown to be independent of wavelength. By retarding the motion of the contact line on the side wall, the contact line friction is thus likely responsible for reducing both the amplitude and, by extension, the wavelength of the buckling along the side wall.

In figure 3, the wavelength of buckling in the bulk and along the sidewalls are shown as a function of the width of the particle-laden interface. The wavelength near the sidewalls remains constant at $\lambda_{\text{wall}} = 1$ mm for all interface widths tested and is not affected by confinement. This observation is intuitive, given that the contact line friction mechanism responsible for the reduction in wavelength near the side walls should not be a function of the width of the particle-laden interface.

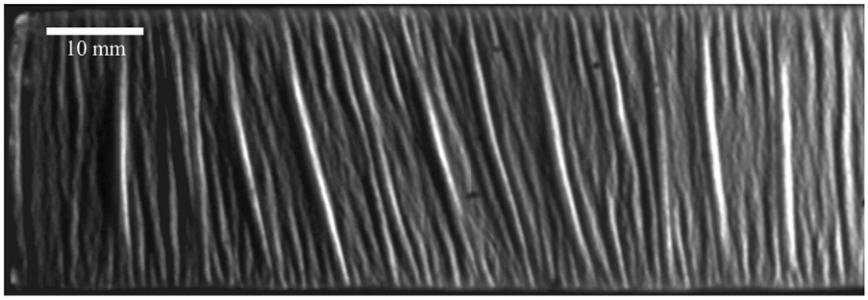

Figure 4. Representative image of a particle-laden interface after the formation of a train of folds. The particle-laden interface was initially 30 mm wide and 125 mm long. Here the surface has been compressed by 25%. Folds are defined area of strain localization bordered by areas of nearly constant strain.

The bulk wavelength, however, is strongly affected by the confinement effects of the side walls. For interfaces with widths greater than 22.5 mm, the wavelength was found to be independent of interface width and approximately $\lambda_{bulk} = 1.8$ mm. This is slightly larger than the value measured by Kassuga and Rothstein [24] for lycopodium powder adsorbed to a water–decane interface and agrees well with measurements of Vella *et al* [10] for lycopodium powder on an air–water interface. This result is expected as the wavelength should scale with the square root of the capillary length. As the confinement is increased and the width reduced below 22.5 mm, the bulk wavelength was found to decrease monotonically, approaching the side wall wavelength as the interface width was reduced to 6.5 mm.

For thin elastic films, cascading has been characterized by an approximately continuous change in wavelength from one part of a sheet to another through a series of transitions where one wrinkle splits into two [26]. The smoothness of the transition between wavelengths can be measured by calculating the average wavelength over a line parallel to the edge of the sheet as a function of the distance, y, from that line to the edge of the sheet [27]. The scaling for wavelength with distance from the edge of the sheet should be [27] :

$$\lambda_{light} \propto y^{2/3} \tag{3}$$

$$\lambda_{heavy} \propto y^{1/2}, \tag{4}$$

where 'light' refers to sheets under negligible lateral tension and 'heavy' refers to sheets under considerable tension. This terminology comes from observations of wavelength variation along hanging drapes and curtains [27]. The tension smoothens out the transition because it makes it energetically unfavorable to focus the curvature on a single point. Therefore, 'heavy' sheets are characterized by smoother transitions than 'light' sheets, as it is reflected on the scaling in equations (3) and (4).

Although cascading has been observed in particle-laden interfaces [24], a large variability in the average wavelength was found across the film and the precise position of the edge of the particle raft was not easily determined. Here the results are much more conducive to analyzing the cascading events as the variation in wavelength from the edge of the sheet can be studied by measuring the wavelength at the center of the sheet as confinement is decreased or by measuring the wavelength as a function of distance from the side walls. Both protocols produce a smooth and consistent transition in buckling wavelength that is fit well by a slope of heavy sheet power law dependence of ½ in equation (4). Thus the influence of the interfacial friction boundary condition is quite strong with an influence which can be seen in figure 2 to extend up to approximately 10 mm or about $5\lambda_{bulk}$ away from the side wall even when the influence of confinement on the bulk wavelength is not observed. These data also are in good agreement with the work of Huang *et al* [26] who demonstrated for a series of thin elastic film floating on a liquid surface, that influence of the interfacial tension at the edge of the film decayed away at a distance of roughly $5\lambda_{bulk}$ from the edge of the film for all film thickness tested.

3.2. Folding of particle-laden interfaces

Unlike wrinkles which are periodic and sinusoidal, folds are characterized by highly-localized surface curvature which is not necessary periodic [38–41]. These strain localizations have been observed in a number of materials under uniaxial and biaxial compression including thin polymer films adhered to soft substrates [38] and floating on liquids [39]. For thin elastic films, the sheet initially buckles. Once buckled, folding has been shown to occur with additional compression once the amplitude of the wrinkles has exceeded roughly one third or more of the initial wavelength of the wrinkling [39, 41]. Folding has been shown to appear as the result of an instability associated with a geometric non-linearity which results in the amplitude of a single wrinkle growing at the expense of those around it [39, 41]. Folding of particle-laden interfaces has not been previously studied in detail, although, it has been observed a number of times in the past [5, 6]. Here we will investigate in detail the transition from wrinkles to folds of particle-laden interfaces.

An example of a folded particle-laden interface is presented in figure 4. In figure 4, the lycopodium covered air–water interface started with initial dimensions of 30 mm wide and 125 mm long and has been compressed by 25%. In this case, wrinkling was found to initiate at approximately 10% compressive strain. Soon thereafter, folds could clearly be observed. In figure 4, the wrinkles appear as strong bright lines across the interface. The onset of folding in this case was at approximately 15% compressive strain. Some variability of about 5% in the critical strain required to wrinkle and fold were

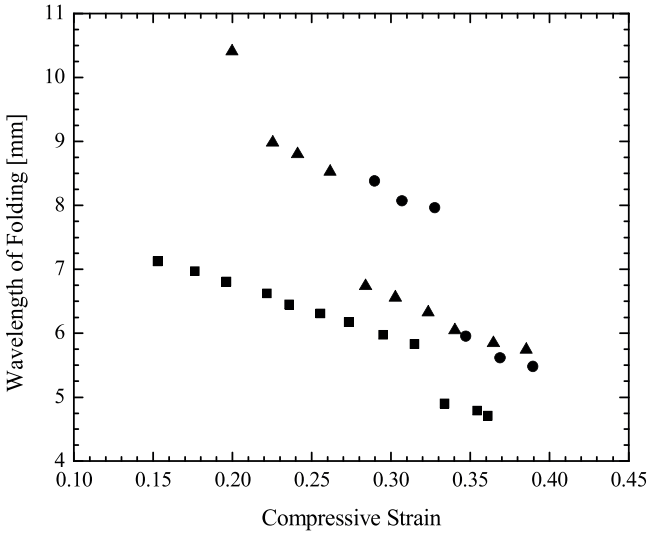

Figure 5. Typical cases of period of folding during stretching as a function of compressive strain for a particle laden interface width of 30 mm. Note each data set is an independent experiment for the same Langmuir trough width. All regions in each data set have the same slope. The discontinuities represent the formation of a new fold which can happen at different strains depending on initial conditions and interface loadings.

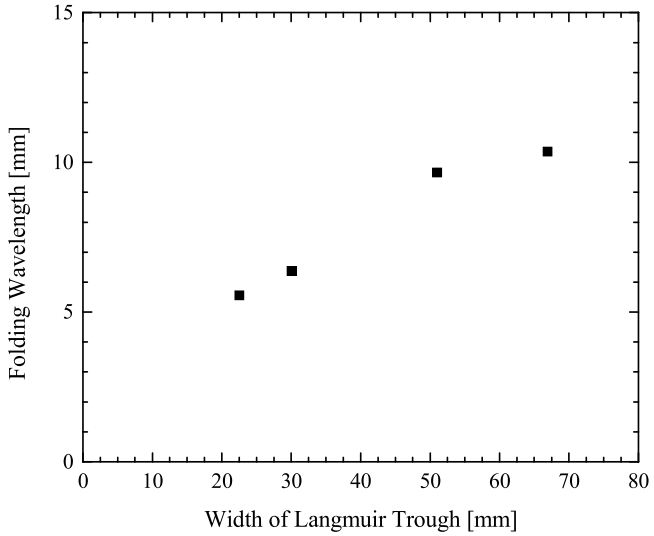

Figure 6. Folding wavelength at 30% strain as a function of the width of the Langmuir trough for a particle-laden interface.

observed from one experiment to the other. This variability was the result of uniformity and density of the initial particle loading on the air–water interface; an experimental challenge that was explored in detail in Kassuga and Rothstein [24]. Once folds developed, strain localization was found to occur, with the wavelength of the surrounding wrinkles remaining constant while the amplitude of the fold can be observed to grow. This observation is consistent with previously observed fold formation of glassy polymers adhered to a soft elastomeric substrate [38], but interestingly these observations are different from the observations of fold formation for thin films floating on liquids where the formation of folds was observed to slowly eliminate the nearby wrinkles [39, 42]. Folds were observed to form either individually or *en masse* in the form of a small train of folds. These trains were found to form with a constant periodicity across the interface. This observation is again consistent with thin elastic films on soft elastomeric substrates and not liquid substrates where single folds and not multiple folds were observed.

In figure 5, the wavelengths of the folds are shown as a function of imposed strain for 30 mm wide particle-laden interface. Below 15% compression, no folds are observed, just wrinkles. Above 15% compression, a series of 14 folds formed *en masse* and were spread nearly uniformly across the interface as seen in figure 4. As the interface was further compressed, the wavelengths of the folds were found to decrease linearly with increasing compressive strain. This is expected as all further compression in the interface was localized as increased amplitude of the folds bringing the folds closer together as the interface was compressed. At 35% compression, a single new fold was observed to appear on the particle-laden interface resulting in a step change in the wavelength of the folds as seen in figure 5. These results, although shown for only one interface condition, were consistent for all the interface widths studied that eventually produced folds.

The effect of interface confinement and the presence of the side walls on the folding of the particle-laden interfaces was also investigated. In figure 6, the period between folds is shown for all of the interface widths studied, 6.5 mm $< W <$ 66.9 mm, at a compressive strain of 30%. As is clearly seen in figure 6, only interfaces with widths between 22.5 and 66.9 mm were found to contain folds. Even at compressive strains in excess of 40%, the formation of folds was not observed for interfaces with widths less than 22.5 mm. Recall, that for widths below 22.5 mm, the wavelength of wrinkling in the bulk was found to be affected by the presence of the side walls and the reduction of the buckling wavelength caused by contact line friction. Note also that a close inspection of figure 4 shows that the folds do not propagate all the way to the wall, but their amplitude is reduced as they approach the wall where it eventually approaches the amplitude of the surrounding wrinkles before splitting in two in order to match the dominant wavelength of wrinkling near the side walls. Thus, it is clear that the same contact line friction that stabilizes the large amplitude wrinkles in favor of lower amplitude and shorter wavelength wrinkles near the wall also inhibits fold formation and growth.

Looking deeper into the data in figure 6 one observes that the wavelength of folding increases monotonically with increasing interface width. Thinking about the data in figure 6 in terms of wavenumber instead of wavelength, the data imply that the 22.5 mm wide interface contained twice as many folds as the 66.9 mm wide interface. One interpretation of this observation is that, as the confinement is reduced, a transition occurs from a regime of multiple folds similar to what has been observed for thin polymer films on soft elastomeric substrates towards the expected solution of a thin film on a liquid interface where a single fold is preferred over multiple folds. This analysis would suggest that strain localization is reduced with reduced confinement resulting in fewer folds. An alternative interpretation is that due to the larger wavelength of the folds compared to wrinkles, the influence of the side walls and

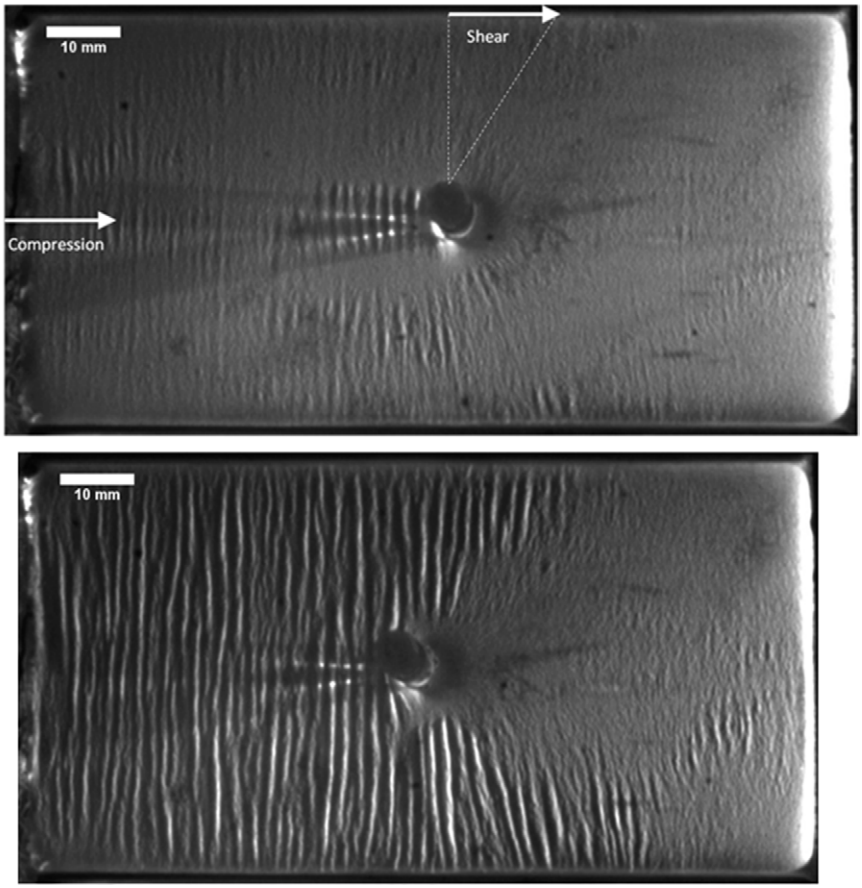

Figure 7. Wrinkling patterns that result from a lycopodium powder covered air–water interface pierced by an immobile 5 mm diameter acrylic cylinder. The cylinder was placed at the center of the 66.9 mm × 125 mm wide particle-laden interface. The compressive strain is introduced by a moving left wall and is increased from 11% (top) to 17% (bottom) in the images presented. The resulting shear strain between the cylinder and the side walls is 44% (top image) and 69% (bottom image).

the cascade of wavelength from the wall extend much deeper into the bulk. As a result, although the effect of the side walls on wrinkles decayed away after about 20 mm, the distance is much larger for the folds. If the same $5\lambda_{\text{fold}}$ is needed to transition from the wavelength of the fold to the reduced wavelength at the edge of the sheet [26], one would expect a plateau in the wavelength of the folds for very wide interfaces, just as was observed for wrinkles in figure 3. In this case, $5\lambda_{\text{fold}} > 55$ mm and a Langmuir trough having a minimum width of 110 mm would be needed to observe the plateau. Unfortunately, our Langmuir trough design was not capable of generating interfaces wide enough to test this hypothesis. Additional evidence that this is indeed a cascading of folds on the particle-laden interface can be acquired from the data in figure 6 as the variation of wavelength with interface width can be fit with power law of ½ indicating heavy sheet behavior as was similarly observed for the wrinkling cascades. These measurements clearly demonstrate that confinement has a large impact on both the wavelength of buckling and folding on a particle-laden interface.

3.3. Buckling around fixed objects

In order to study the impact of shear on the buckling of particle-laden interfaces, shear was purposefully reintroduced into the Langmuir trough by inserting a series of immobile obstacles through the particle-laden interface at its center as shown schematically in figure 1. As described in section 2, these objects included an acrylic circular cylinder with a diameter of 5 mm and an acrylic rectangular prism with cross section of 3 mm × 10 mm. All experiments were performed with the widest interface possible, $w = 66.9$ mm, to try to minimize the influence of the side walls.

In figure 7, the wrinkling patterns around a circular cylinder sticking through the particle-laden interface are shown for two different global compressive strains, 11% and 17%, while a additional shear strain of 44% and 69% is produced between the stationary circular cylinder and the moving side wall of the Langmuir trough. A number of observations can be quickly made from the buckling patterns and their orientation across the film. First, one notes that at 11% compression, buckling was not observed on the particle-laden interfaces in the absence of the object piercing the interface. The observation of buckling at 11% strain is therefore a direct result of the presence of the obstacle. At 11% strain, buckling is most pronounced in regions upstream of the cylinder, between the cylinder and the moving wall. In this region, the local compressive strain is twice as large as the globally imposed compressive strain because the presence of the stationary cylinder essentially cuts the length of the interface in half along the

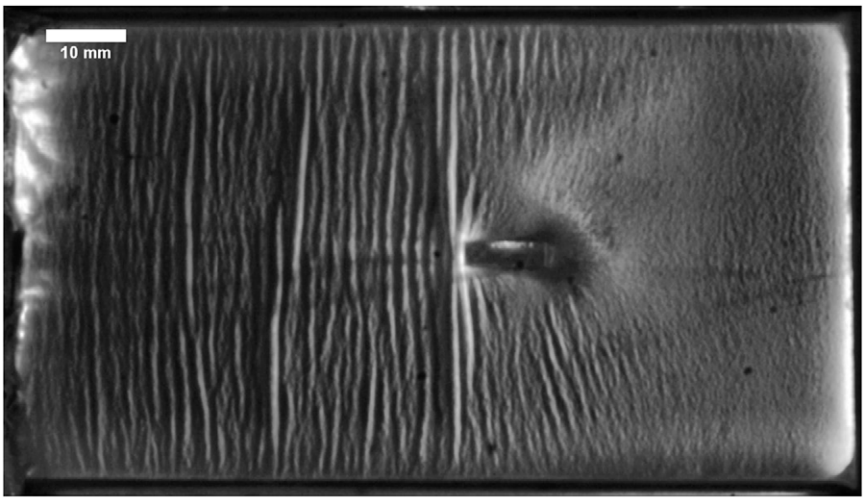

Figure 8. Wrinkling patterns that result from a lycopodium powder covered air–water interface pierced by an immobile rectangular prism with a cross section of 3 mm × 10 mm. The rectangular prism was placed at the center of the 66.9 mm × 125 mm wide particle-laden interface with its long side aligned with the compression direction. The compressive strain is introduced by a moving left wall and is 23% and the shear strain between the side walls and the rectangular prism is 90%.

midplane. As the strain is increased to 17%, buckling and folding of the interface are observed over the entire particle-laden interface upstream of the cylinder. At this compressive strain, buckling is expected everywhere along the interface, but in figure 7 there are clearly regions downstream of the cylinder where no buckling was observed. In these unbuckled regions, the presence of the cylinder has shielded the interface from significant compression. The shielded regions are not limited to the interface directly behind the cylinder, where the compressive strain should be negligible, but was found to extend downstream and spread away from the cylinder at an angle close to 45°. Recent measurements of 2D granular media flowing around an obstacle have shown similar shielding effects [43, 44]. In their measurements, Kolb *et al* [43, 44] showed that the packing density of the granular media increased upstream of the obstacle and was reduced downstream of the obstacle. In some cases, a cavity devoid of particles was observed downstream of the obstacle. Although no such cavity was observed here, a clear difference in particle packing and interface compression is evident by the variations in interface patterns.

Since the side walls are deforming affinely with global compressive strain, the interface very near the side walls is expected to buckle at 17% strain as it experiences the full strain imposed on the interface. In fact, it is only very near the walls that the global strain is actually imposed. The compressive strain varies all along the interface going from 34% directly upstream of the cylinder, to 0% directly downstream of the cylinder and 17% along the side walls. Additionally, the presence of the cylinder provides a shear stress/strain along the interface between the cylinder and the side walls as the interface moves with the side walls and is fixed at the cylinder. The buckling pattern around the cylinder, especially in the regions of closest confinement with the side walls shows evidence of these shear effects as the wrinkles are no longer oriented normal to the compression direction, but have rotated inward towards the centerline downstream of the cylinder. Even in a pure shear flow, the interface would still experience compression at an angle 45° to the shear direction which could lead to interface buckling. The angle of rotation of the buckling can be used to determine the principal compression direction and calculate the relative magnitude of compressive and shear strain along the interface.

In figures 8–10, the acrylic cylinder is replaced by an acrylic rectangular prism that pierces the particle-laden interface with a cross section of 3 mm × 10 mm. Here we vary the orientation of the rectangular prism. In figure 8, the rectangular prism is aligned with the long axis of the rectangle in the compression direction. In figure 9, the rectangle is aligned at 45° and in figure 10 the long axis of the rectangle is aligned at 90° to the compression direction. When compared with the cylinder in figure 7, the presence of the immobile rectangle piercing the lycopodium particle-laden interface presents very similar buckling and folding patterns across the interface: both the rectangular prism and the circular cylinder wrinkled at low global strains (~10%) in the region just upstream of the obstacle; a shielding of the interface and a prevention of buckling downstream of the obstacle was observed in both cases; and a shear-induced rotation of the buckling patterns between the obstacle and the side wall was present for interfaces pierced by both rectangular prisms and cylinders. The major difference in the buckling patterns can be traced to the presence of the flat edges and sharp corners of the rectangular prism. The long flat edges of the rectangular prism appear to be more efficient at orienting and aligning the wrinkles parallel to the surface of the rectangle than the circular cylinder. In fact, the shear introduced by the presence of the rectangular prism results in the early onset of strong, deep folds very close to the surface of the rectangular prism. These folds are seen to wrap around the corners of the rectangle and realign with the adjacent wall of the rectangular prism, especially in the case with 45° alignment. Thus, although the circular cylinder and the rectangular prism have a similar impact on buckling, the presence of the sharp corners and the long flat sides of the

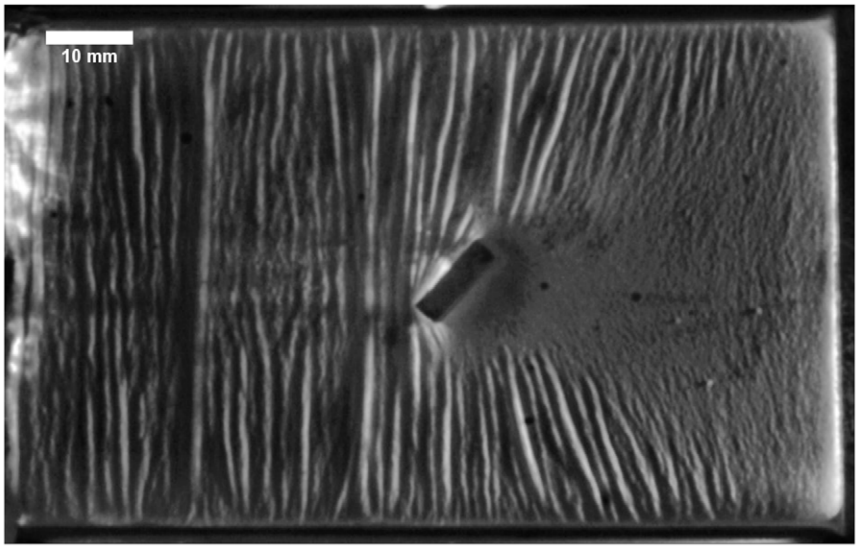

Figure 9. Wrinkling patterns that result from a lycopodium powder covered air–water interface pierced by an immobile rectangular prism with a cross section of 3 mm × 10 mm. The rectangular prism was placed at the center of the 66.9 mm × 125 mm wide particle-laden interface with its long side aligned at a 45° angle with the compression direction. The compressive strain is introduced by a moving left wall and is 31% and the shear strain between the side walls and the rectangular prism is 120%.

Figure 10. Wrinkling patterns that result from a lycopodium powder covered air–water interface pierced by an immobile rectangular prism with a cross section of 3 mm × 10 mm. The rectangular prism was placed at the center of the 66.9 mm × 125 mm wide particle-laden interface with its long side aligned at a 90° angle with the compression direction. The compressive strain is introduced by a moving left wall and is 16% and the shear strain between the side walls and the rectangular prism is 70%.

rectangular prism appear to enhance strain localization and the transition from wrinkles to folds along the interface.

4. Conclusions

In this paper, we investigated the buckling of an air–water interface populated by 31 micron lycopodium powder particles using a modified Langmuir trough. The specially designed Langmuir trough had side walls that deformed affinely with the particle-laden interface in order to minimize the effect of shear during interface compression. The effect of interface width and confinement effects from the side walls were studied by systematically reducing the width of the Langmuir trough and measuring the buckling wavelength at various locations across the interface. For interfaces wider than 20 mm, the bulk wavelength was found to be independent of interface width. However, for interface widths less than 20 mm, the bulk wavelength was found to decrease and approach the wavelength observed near the side walls. We postulate that due to contact line friction, the amplitude and wavelength of the wrinkles near the side walls were reduced by a factor two in comparison to the unconfined wavelength in the bulk. For thin polymer films, the added force of surface tension has been shown to have a similar effect on wavelength. A cascade in wavelength was observed as one moved out from the center of the particle-laden interface towards the sidewalls similar to what has been observed in thin polymer films floating on a liquid interface. The wavelength at the walls was not affected by confinement. However, for Langmuir trough with widths smaller than 20 mm, the bulk wavelength was found to decrease, eventually approaching the wavelength at the side walls for highly confined films.

At large interface compressions, a transition from wrinkles to folds was observed. These folds represent a strain localization and as a result the wavelength of wrinkles between folds was not found to change with increasing interface compression just the wavelength of the folds. Confinement was also found to have an impact on folding. Below an interface width of 20 mm, no fold were observed. For particle-laden interfaces wider than 20 mm, folds were observed with the number of folds increasing and the wavelength between folds decreasing with increasing confinement. These observations mirrored the observation for wrinkling wavelength and demonstrated that confinement has a large impact on both buckling and folding of a particle-laden interface.

Once the effects of shear had been removed, a series of experiments were designed to systematically reintroduce shear onto the particle-laden interface. To study the effect of shear, a series of immobile objects including circular cylinders and rectangular prisms were placed through the center of the particle-laden interface before compression. These objects were found to enhance wrinkling and folding upstream of the object, eliminate wrinkling and folding in and expanding region downstream of the object and through the shear strain introduced by the moving sidewalls and the immobile obstacle, realign the wrinkles along the side of the immobile obstacles. The sharp corners and long flat sidewalls of the rectangular prism were found to be more efficient at aligning the wrinkles and served as a nucleation site for folds at strains just beyond the onset of wrinkling.

Acknowledgments

The authors would like to thank the National Science Foundation for support of this research through the Materials Research Science and Engineering Center on Polymers (DMR-0820506) at the University of Massachusetts.

References

[1] Binks B P 2002 *Curr. Opin. Colloid Interface Sci.* **7** 21
[2] Pickering S U 1907 *J. Chem. Soc., Trans.* **91** 2001
[3] Binks B P and Lumsdon S O 1999 *Phys. Chem. Chem. Phys.* **1** 3007
[4] Ashby N P and Binks B P 2000 *Phys. Chem. Chem. Phys.* **2** 5640
[5] Edmond K V, Marquez M, Schofield A B, Rothstein J P and Dinsmore A D 2006 *Langmuir* **22** 9052
[6] Mulligan M and Rothstein J P 2011 *Langmuir* **27** 9760
[7] Dinsmore A D, Hsu M F, Nikolaides M G, Marquez M, Bausch A R and Weitz D A 2002 *Science* **298** 1006
[8] Boneva M P, Christov N C, Danov K D and Kralchevsky P A 2007 *Phys. Chem. Chem. Phys.* **9** 6371
[9] Oettel M and Dietrich S 2008 *Langmuir* **24** 1425
[10] Vella D, Aussillous P and Mahadevan L 2004 *Europhys. Lett.* **68** 212
[11] Zeng C, Bissig H and Dinsmore A D 2006 *Solid State Commun.* **139** 547
[12] Daniello R, Donnell M, Khan K and Rothstein J P 2014 *Phys. Rev.* E **89** 023014
[13] Vella D and Mahadevan L 2005 *Am. J. Phys.* **73** 817
[14] Cavallaro M, Botto L, Lewandowski E P, Wang M and Stebe K J 2011 *Proc. Natl Acad. Sci.* **108** 20923
[15] Poty M, Lumay G and Vandewalle N 2014 *New J. Phys.* **16** 023013
[16] Kralchevsky P A and Nagayama K 2000 *Adv. Coll. Int. Sci.* **85** 145
[17] Nikolaides M G, Bausch A R, Hsu M F, Dinsmore A D, Brenner M P, Gay C and Weitz D A 2002 *Nature* **420** 299
[18] Reynaert S, Moldenaers P and Vermant J 2006 *Langmuir* **22** 4936
[19] Aveyard R, Clint J H, Nees D and Paunov V N 2000 *Langmuir* **16** 1969
[20] Moncho-Jorda A, Martínez-Lopez F, Gonzalez A E and Hidalgo-Alvarez R 2002 *Langmuir* **18** 9183
[21] Pieranski P 1980 *Phys. Rev. Lett.* **45** 569
[22] Monteux C, Kirkwood J, Xu H, Jung E and Fuller G G 2007 *Phys. Chem. Chem. Phys.* **9** 6344
[23] Monteux C, Jung E and Fuller G G 2007 *Langmuir* **23** 3975
[24] Kassuga T D and Rothstein J P 2015 *J. Colloid Int. Sci.* **448** 287
[25] Planchette C, Lorenceau E and Biance A-L 2012 *Soft Matter* **8** 2444
[26] Huang J, Davidovitch B, Santangelo C D, Russell T P and Menon1 N 2010 *Phys. Rev. Lett.* **105** 038302
[27] Vandeparre H, Piñeirua M, Brau F, Roman B, Bico J, Gay C, Bao W, Lau C N, Reis P M and Damman P 2011 *Phys. Rev. Lett.* **106** 224301
[28] Cicuta P and Vella D 2009 *Phys. Rev. Lett.* **102** 138302
[29] Aumaitre E, Vella D and Cicuta P 2011 *Soft Matter* **7** 2530
[30] Davidovitch B 2009 *Phys. Rev.* E **80** 025202
[31] Davidovitch B, Schroll R D, Vella D, Adda-Bedia M and Cerda E A 2011 *Proc. Natl Acad. Sci.* **108** 18227
[32] Huang J, Juszkiewicz M, Jeu W H d, Cerda E, Emrick T, Menon N and Russell T P 2007 *Science* **317** 650
[33] Pineirua M, Tanaka N, Roman B and Bico J 2013 *Soft Matter* **9** 10985
[34] Roman B and Bico J 2010 *J. Phys.: Condens. Matter* **22** 493101
[35] Zeng C, Brau F, Davidovitch B and Dinsmore A D 2012 *Soft Matter* **8** 8582
[36] de Gennes P G, Brochard-Wyart F and Quéré D 2004 *Capillarity and Wetting Phenomena: Drops, Bubbles, Pearls, Waves* (New York: Springer)
[37] Gao L and McCarthy T J 2006 *Langmuir* **22** 6234
[38] Ebata Y, Croll A B and Crosby A J 2012 *Soft Matter* **8** 9086
[39] Pocivavsek L, Dellsy R, Kern A, Johnson S, Lin B, Lee K Y C and Cerda E 2008 *Science* **320** 912
[40] Diamant H and Witten T A 2011 *Phys. Rev. Lett.* **107** 164302
[41] Oshri O, Brau F and Diamant H 2015 *Phys. Rev.* E **91** 052408
[42] King H, Schroll R D, Davidovitch B and Menon N 2012 *Proc. Natl. Acad. Sci.* **109** 9716
[43] Kolb E, Cixous P and Charmet J C 2014 *Granular Matter* **16** 223
[44] Kolb E, Cixous P, Gaudouen N and Darnige T 2013 *Phys. Rev.* E **87** 032207